Decoherence of a charge qubit embedded inside a suspended phonon cavity

Y. Y. Liao,[1,*] Y. N. Chen,[2] W. C. Chou,[1] and D. S. Chuu[1]
[1]*Department of Electrophysics, National Chiao-Tung University, Hsinchu 300, Taiwan*
[2]*Department of Physics and National Center for Theoretical Sciences, National Cheng-Kung University, Tainan 701, Taiwan*
(Received 11 July 2007; published 14 January 2008)

This study elucidates the theory of phonon-induced decoherence of a double dot charge qubit that is embedded inside a suspended semiconductor slab. The influences of the lattice temperature, width of the slab, and positions of the dots on the decoherence are analyzed. Numerical results indicate that the decoherence in the slab system is weaker than that in a bulk environment. In particular, the decoherence is markedly suppressed by the inhibition of the electron-phonon coupling. Such a system with low decoherence may be useful for manipulating the qubits.

DOI: 10.1103/PhysRevB.77.033303 PACS number(s): 73.21.La, 63.20.K−, 03.65.Yz, 62.25.−g

Various candidates for building blocks of quantum computers have been proposed[1–4] and demonstrated[5–8] using nanoscale solid state structures. Among them, the semiconductor double quantum dot (DQD) is a prototype of a solid state qubit, which comprises a pair of quantum dots connected through an interdot tunneling barrier.[9] The DQD acts as a two-level system when at most one excess electron is allowed in the double dot potential.[10] The two logical states correspond to the localized states of the excess electron in one or the other dot. Accordingly, the state of the charge qubit can be expressed as a linear superposition of the two localized states, and has recently been demonstrated in a GaAs/AlGaAs heterostructure.[6,7] An important advantage of this system is that all of the qubit parameters can be controlled by varying the external gate voltages. Furthermore, it may have great potential for scalability and integration with current microelectronic technologies.

However, various mechanisms may destroy the coherence of the system since the charge qubit can never be isolated completely from its environment.[6] The electron-phonon interaction is one possible decoherence channel and has been theoretically investigated. It ranges from a single charge qubit[11–16] to two coupled charge qubits.[17] Although many works have focused on bulk cases, the decoherence of a charge qubit in a confined structure has received little attention. Unlike bulk material, the confined structure supports the tailoring of the phonon density of states by altering the dimensions.[18–21] Therefore, the charge qubit in a confined structure is expected to exhibit some interesting characteristics.

This work investigates the decoherence of a DQD qubit that is embedded inside a suspended semiconductor slab. To study the decoherence of the qubit, the master equation is solved under the Born-Markov approximation.[22–24] The qubit of higher quality is found in the slab system. In particular, the decoherence is dramatically suppressed by the inhibition of the electron-phonon coupling, suggesting that a robust DQD qubit can be achieved in a suspended structure.

Consider the setup shown in Fig. 1, in which a single electron is confined in a GaAs double dot structure that is embedded inside a freestanding slab. With advances in novel nanofabrication technology, quantum dots can now be embedded into the suspended structure.[20,21] Most of the structure is spatially separated from most of the substrate such that the acoustic modes between the surfaces can be ideally and completely confined. The in-plane scale is assumed to exceed substantially the width and dot size. If the effect of the contact with the semiconductor substrate (distortion of the acoustic vibrations) is neglected, then the slab is just like a cavity.[19] Before the calculation, the relative importance of piezoelectric potential and deformation potential is determined. The ratio of the piezoelectric potential strength to the deformation potential strength depends on $(ee_{14}/E_a q)^2$, where e is the electronic charge, e_{14} is the piezoelectric constant, E_a is the deformation potential constant, and q is the wave vector.[25,26] In bulk GaAs systems, piezoelectric interaction normally prevails for long-wavelength acoustic phonons.[14,15] In a phonon cavity, however, the confinement yields a lower bound on the wavelength, and this cuts off phonons with low momenta that determine the strength of the piezoelectric electron-phonon coupling. Thus, deformation potential can be argued to be the main contributor to confined phonon geometries.[18,19]

The Hamiltonian of this model is written as $H=H_e+H_p+H_{ep}$, corresponding to the electron Hamiltonian, the phonon Hamiltonian, and electron-phonon interaction, respectively. Based on the basis of two localized states, $|L\rangle$ and $|R\rangle$, the electron Hamiltonian in a DQD is given by

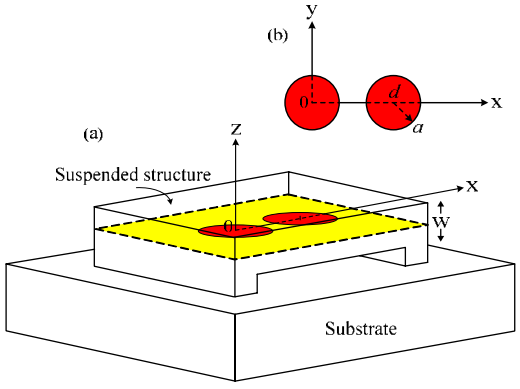

FIG. 1. (Color online) (a) Schematic view of a DQD embedded in a suspended semiconductor slab with a width of w. The surfaces of the slab are $z=\pm w/2$, and the dots are located at $z=0$. (b) The top view shows that two identical dots are performed with the dot radii of a and interdot distance of d.

$$H_e = \frac{\varepsilon}{2}\sigma_z + \Delta\sigma_x, \tag{1}$$

where $\sigma_{x,z}$ are Pauli matrices, ε is the level difference, and Δ is the tunneling coupling between the dots. The parameters ε and Δ can be experimentally controlled through external gate voltages.[6,7] The phonon Hamiltonian for the slab is

$$H_p = \sum_{\mathbf{q}_\parallel,n} \hbar\omega_{\mathbf{q}_\parallel,n} b^\dagger_{\mathbf{q}_\parallel,n} b_{\mathbf{q}_\parallel,n}, \tag{2}$$

where $\omega_{\mathbf{q}_\parallel,n}$ is the frequency and $b^\dagger_{\mathbf{q}_\parallel,n}$ ($b_{\mathbf{q}_\parallel,n}$) is the creation (annihilation) operator of the phonon, respectively, characterized by the in-plane wave vector $\mathbf{q}_\parallel$ and the branch n.

To calculate the phonon dispersion relations, one has to study the acoustic phonon quantization in an infinite film with width w (Fig. 1). The starting point is the elastic continuum model of acoustic phonons. In this model, the elastic properties of the slab are assumed to be isotropic. Small elastic vibrations of a solid slab can then be defined by the displacement vector $\mathbf{u}$. Under the isotropic elastic continuum approximation, the equation for the displacement vector $\mathbf{u}$ can be written as[27]

$$\frac{\partial^2\mathbf{u}}{\partial t^2} = c_t^2\nabla^2\mathbf{u} + (c_l^2 - c_t^2)\,\nabla\,(\nabla\cdot\mathbf{u}), \tag{3}$$

where c_l and c_t are the velocities of longitudinal and transverse bulk acoustic waves. To define a system of confined modes, Eq. (3) should be complemented by the boundary conditions at the slab surface $z=\pm w/2$. Due to the confinement, phonons will be quantized in subbands. For each in-plane component $q_\parallel$, there are infinitely many subbands. Since we consider only the deformation potential, there are two confined acoustic modes: dilatational waves and flexural waves. Shear waves are neglected because of their vanishing interaction with the electron. The dispersion relations for two waves are described by[18]

$$\omega^2_{\mathbf{q}_\parallel,n} = c_l^2(q_\parallel^2 + q_{l,n}^2) = c_t^2(q_\parallel^2 + q_{t,n}^2), \tag{4}$$

where $q_{l,n}$ and $q_{t,n}$ can be determined from the equations

$$\frac{\tan q_{t,n}w/2}{\tan q_{l,n}w/2} = -\frac{4q_\parallel^2 q_{l,n}q_{t,n}}{(q_\parallel^2 - q_{t,n}^2)^2} \tag{5}$$

and

$$\frac{\tan q_{l,n}w/2}{\tan q_{t,n}w/2} = -\frac{4q_\parallel^2 q_{l,n}q_{t,n}}{(q_\parallel^2 - q_{t,n}^2)^2} \tag{6}$$

for the dilatational and flexural waves, respectively. Moreover, the electron-phonon interaction is written as[10]

$$H_{ep} = \frac{\sigma_z}{2}\sum_{\substack{\mathbf{q}_\parallel,n\\ i=d,f}} g^i_{\mathbf{q}_\parallel,n}(b^\dagger_{\mathbf{q}_\parallel,n} + b_{-\mathbf{q}_\parallel,n}), \tag{7}$$

with $g^i_{\mathbf{q}_\parallel,n} = \lambda_{i,n}P(\mathbf{q}_\parallel)(1-e^{-i\mathbf{q}_\parallel\cdot\mathbf{d}})$. The function $\lambda_{i,n}$ describes the intensity of the electron interacting with the dilatational waves,

$$\lambda_{d,n}(\mathbf{q}_\parallel) = F_{d,n}\sqrt{\frac{\hbar E_a^2}{2A\rho\omega_{\mathbf{q}_\parallel,n}}}(q_{t,n}^2 - q_\parallel^2)(q_{l,n}^2 + q_\parallel^2) \times\sin\left(\frac{wq_{t,n}}{2}\right)\cos(q_{l,n}z), \tag{8}$$

and with the flexural waves,

$$\lambda_{f,n}(\mathbf{q}_\parallel) = F_{f,n}\sqrt{\frac{\hbar E_a^2}{2A\rho\omega_{\mathbf{q}_\parallel,n}}}(q_{t,n}^2 - q_\parallel^2)(q_{l,n}^2 + q_\parallel^2) \times\cos\left(\frac{wq_{t,n}}{2}\right)\sin(q_{l,n}z), \tag{9}$$

where $F_{d,n}$ ($F_{f,n}$) is the normalization constant, A is the area of the slab, and ρ is the mass density. The dot form factor is

$$P(\mathbf{q}_\parallel) = \int n(\mathbf{r}_\parallel)e^{-i\mathbf{q}_\parallel\cdot\mathbf{r}_\parallel}d^3\mathbf{r}. \tag{10}$$

Here, the charge density distribution on the dot $n(\mathbf{r}_\parallel)$ is assumed to be Gaussian in the xy plane and localized in the z direction. Correspondingly, the form factor reads $P(\mathbf{q}_\parallel) = \exp[-(\mathbf{q}_\parallel a)^2/2]$.[14,15] It is worth noting that the parameters $(q_\parallel, q_{l,n}, q_{t,n})$ of dilatational and flexural waves independently satisfy the dispersion relations. In general, both waves are contributive. However, one can consider only the dilatational wave for simplicity if the dots are located in the center of the slab ($z=0$). This is because the function $\lambda_{f,n}$ for flexural waves plays no role.

To investigate the decoherence of the qubit, we solve the master equation in the Born-Markov approximation.[22–24] The system and phonon bath are assumed to be isolated at $t=0$. Accordingly, the density matrix $\rho(t)$ is

$$\dot\rho(t) = \frac{i}{\hbar}[\rho(t), H_e] - \frac{1}{\hbar^2}\int_0^t dt'\{[S,\tilde S(t'-t)\rho(t)]K(t-t') - [S,\rho(t)\tilde S(t'-t)]K(t-t')^*\}, \tag{11}$$

where $S=\sigma_z/2$ is the system part of Eq. (7) with its interaction representation $\tilde S$. The correlation function of the environment K is written as

$$K(t) = \int_0^\infty d\omega J(\omega)\left[\cos(\omega t)\coth\left(\frac{\hbar\omega}{2k_BT}\right) - i\sin(\omega t)\right], \tag{12}$$

with Boltzmann constant k_B, temperature T, and $K(-t) = K(t)^*$. The spectral density of the phonon bath for the slab is defined according to

$$J(\omega) = \sum_{\substack{\mathbf{q}_\parallel,n\\ i=d,f}} |g^i_{\mathbf{q}_\parallel,n}|^2\delta(\omega - \omega_{\mathbf{q}_\parallel,n}). \tag{13}$$

In the recent experiment by Hayashi *et al.*,[6] the electron is initially in the left dot. If the tunneling coupling is turned on, the electron can tunnel resonantly back and forth between two dots under the condition of $\varepsilon=0$. To be close to the experimental situation, we can simplify the master equation.

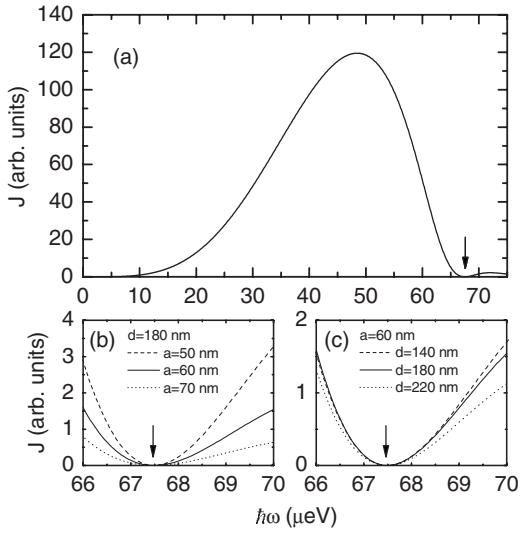

FIG. 2. (a) Phonon spectral density J as a function of energy $\hbar\omega$ for dot radius $a=60$ nm and interdot distance $d=180$ nm. The results of different geometric parameters are plotted for fixed (b) $d=180$ nm and (c) $a=60$ nm, respectively. It is found that a suppressed spectral density can occur (arrows).

Following the standard treatment, the population of the left-dot state is written as

$$n_L(t) \cong \frac{1}{2}[1 + e^{-t/T_d}\cos(\omega t)], \tag{14}$$

with the population $n_R(t)=1-n_L(t)$ for the right-dot state. Further analyzing the parameters, one finds that the decoherence time is $T_d=4\hbar^2/[\pi J(2\Delta/\hbar)\coth(\Delta/k_BT)]$ and the tunneling coupling mainly determines the oscillation frequency $\omega\cong 2\Delta/\hbar$. From the evolution, it is evidently shown that the oscillation of the population will be damped by decoherence. In the course of manipulation, two parameters strongly influence the quality of the qubit. Therefore, we introduce the quality factor Q $(=\omega T_d/2\pi)$ to quantify the loss within the decoherence time.[14–16]

In the following, we address the experimental parameters of the dot radius $a=60$ nm and the interdot distance $d=180$ nm.[28] The material parameters for GaAs quantum dot are $E_a=2.2\times10^{-18}$ J, $\rho=5.3\times10^3$ Kg/m^3, $c_t=3.0\times10^3$ m/s, and $c_l=5.2\times10^3$ m/s.[25] We first analyze the characteristics of the slab with width 130 nm.[20,21] The dots are assumed to be located in the center of the slab. Figure 2(a) shows the spectral density of the confined phonons. In small and large energy regimes, the values are relatively small. This implies that the influence of phonon cavity is weak in these regimes. In addition, we obtain a suppressed spectral density $(J\to 0)$ at certain frequency (arrow). By analyzing the components of Eq. (13), the suppressed phenomenon is unaffected by the geometric parameters of the dots. As can be seen in Figs. 2(b) and 2(c), the suppressed point is independent of the dot size and interdot distance (arrows). At this point, a vanishing divergence of displacement field $\mathbf{u}$ can be found such that the electron-phonon interaction becomes ineffective.[19,29]

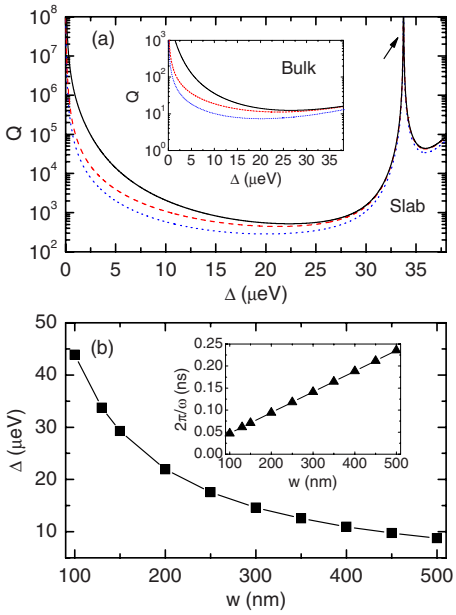

FIG. 3. (Color online) (a) Quality factor Q as a function of tunneling coupling Δ for slab and bulk systems (upper inset). The temperatures are $T=20$ mK (black solid line), 200 mK (red dashed line), and 400 mK (blue dotted line), respectively. A drastic enhancement of quality factor is found to be independent of temperature (arrow). (b) Dependence of the specific tunneling couplings Δ for perfect quality factor on the width w. The corresponding period of time-dependent population is shown in the lower inset.

Figure 3(a) shows the high quality factor of the qubit as a function of tunneling coupling. With the increase of the tunneling coupling, the minimal value remains ten times higher than that in a bulk environment (upper inset). In most cases, the quality factor is several orders of magnitude higher than that in the bulk case. This result indicates that such a system has relatively smaller decoherence. Most important of all, a perfect quality factor $(Q\to\infty)$, which is independent of temperature, is found around $\Delta\approx 33.7$ μeV (arrow). One can expect that, at this point, the coherence of the qubit, indeed, is long kept without losses. This can be understood by the fact that the particular phonon modes of the slab give rise to drastic suppression of J as shown in Fig. 2. To learn more about the characteristic of the slab, in Fig. 3(b) we plot the required tunneling coupling to achieve a perfect quality factor for different widths of the slabs. It is clearly shown that a smaller tunneling coupling is required for a wider slab. Correspondingly, the system has a larger period of the oscillation between two states (lower inset).

Let us now turn to the discussions on the quality factor for different positions of the dots. As shown in Fig. 4, if the dots are far away from the center, the flexural waves actually contribute to the decoherence channel. Correspondingly, a reduced quality factor is found with the increase of the tunneling coupling, and the influence becomes apparent in small and large tunneling coupling regimes. This is due to the competitions between dilatational and flexural waves. As can be seen in the inset, the total spectral density contains two components: dilatational and flexural parts. It is clearly shown

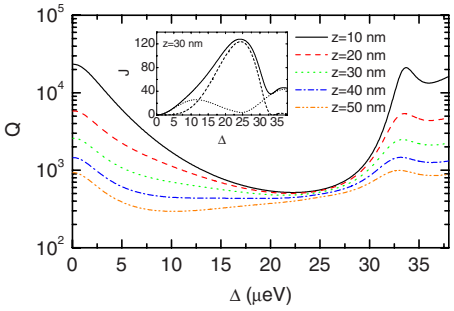

FIG. 4. (Color online) Quality factor Q as a function of tunneling coupling Δ for different vertical positions of the dots z. The inset shows that the total spectral density (solid line) contains the contributions from the dilatational wave (dashed line) and the flexural wave (dotted line) for $z=30$ nm.

that the flexural wave is dominant in small and large tunneling coupling regimes. Different from the bulk system, the dominant contributor of the decoherence can be transferred between two waves by varying the tunneling coupling. It is also worth mentioning that the condition for perfect quality factor strongly depends on the positions of the system. For example, the quality factor becomes of the order of 10^3 as tunneling coupling $\Delta \approx 33.7$ μeV and vertical position $z=30$ nm. Although the value is no longer infinite, it is still high enough in comparison with bulk system.

A few remarks regarding the comparison of our model with the related work should be made here. For instance, a measure based on the norm of the deviation of the density matrix has been used to quantify decoherence at the NOT gate and the π gate.[30] A spherically symmetric charge distribution is assumed therein, while the model herein assumes a two-dimensional pancake form. The most important difference is that the phonon environment with restricted geometry is considered herein. We believe that if our model is analyzed using the approach presented elsewhere,[30] then the suppressed decoherence should become evident.

In summary, the decoherence of a double dot qubit embedded inside a semiconductor suspended slab was studied. Particular phonon modes can significantly suppress the decoherence, and a qubit with high quality can be achieved. We suggest that such a system is useful for the performance of qubit manipulations.

This work is supported partially by the National Center for Theoretical Sciences and the National Science Council, Taiwan under the Grants Nos. NSC 94-2112-M009-024, NSC 95-2119-M-009-030, and NSC 95-2112-M-006-31-MY3.

*yyliao@mail.nctu.edu.tw

[1] D. Loss and D. P. DiVincenzo, Phys. Rev. A **57**, 120 (1998).
[2] B. E. Kane, Nature (London) **393**, 133 (1998).
[3] Y. Makhlin, G. Schön, and A. Shnirman, Nature (London) **398**, 305 (1999).
[4] T. Tanamoto, Phys. Rev. A **61**, 022305 (2000).
[5] Y. Nakamura, Y. A. Pashkin, and J. S. Tsai, Nature (London) **398**, 786 (1999).
[6] T. Hayashi, T. Fujisawa, H. D. Cheong, Y. H. Jeong, and Y. Hirayama, Phys. Rev. Lett. **91**, 226804 (2003).
[7] J. R. Petta, A. C. Johnson, C. M. Marcus, M. P. Hanson, and A. C. Gossard, Phys. Rev. Lett. **93**, 186802 (2004).
[8] J. Gorman, D. G. Hasko, and D. A. Williams, Phys. Rev. Lett. **95**, 090502 (2005).
[9] W. G. van der Wiel, S. De Franceschi, J. M. Elzerman, T. Fujisawa, S. Tarucha, and L. P. Kouwenhoven, Rev. Mod. Phys. **75**, 1 (2003).
[10] T. Brandes and T. Vorrath, Phys. Rev. B **66**, 075341 (2002).
[11] L. Fedichkin and A. Fedorov, Phys. Rev. A **69**, 032311 (2004).
[12] V. N. Stavrou and X. Hu, Phys. Rev. B **72**, 075362 (2005).
[13] Z. J. Wu, K. D. Zhu, X. Z. Yuan, Y. W. Jiang, and H. Zheng, Phys. Rev. B **71**, 205323 (2005).
[14] S. Vorojtsov, E. R. Mucciolo, and H. U. Baranger, Phys. Rev. B **71**, 205322 (2005).
[15] M. Thorwart, J. Eckel, and E. R. Mucciolo, Phys. Rev. B **72**, 235320 (2005).
[16] U. Hohenester, Phys. Rev. B **74**, 161307(R) (2006).
[17] M. J. Storcz, U. Hartmann, S. Kohler, and F. K. Wilhelm, Phys. Rev. B **72**, 235321 (2005).
[18] N. Bannov, V. Aristov, V. Mitin, and M. A. Stroscio, Phys. Rev. B **51**, 9930 (1995).
[19] S. Debald, T. Brandes, and B. Kramer, Phys. Rev. B **66**, 041301(R) (2002).
[20] E. M. Höhberger, T. Krämer, W. Wegscheider, and R. H. Blick, Appl. Phys. Lett. **82**, 4160 (2003).
[21] E. M. Weig, R. H. Blick, T. Brandes, J. Kirschbaum, W. Wegscheider, M. Bichler, and J. P. Kotthaus, Phys. Rev. Lett. **92**, 046804 (2004).
[22] A. J. Leggett, S. Chakravarty, A. T. Dorsey, M. P. A. Fisher, A. Garg, and W. Zwerger, Rev. Mod. Phys. **59**, 1 (1987).
[23] W. T. Pollard and R. A. Friesner, J. Chem. Phys. **100**, 5054 (1994).
[24] U. Weiss, *Quantum Dissipative Systems* (World Scientific, Singapore, 1999).
[25] H. Bruus, K. Flensberg, and H. Smith, Phys. Rev. B **48**, 11144 (1993).
[26] G. D. Mahan, *Many-Particle Physics* (Plenum, New York, 1990).
[27] B. A. Auld, *Acoustic Fields and Waves* (Wiley, New York, 1973).
[28] H. Jeong, A. M. Chang, and M. R. Melloch, Science **293**, 2221 (2001).
[29] Y. Y. Liao, Y. N. Chen, D. S. Chuu, and T. Brandes, Phys. Rev. B **73**, 085310 (2006).
[30] L. Fedichkin and V. Privman, arXiv:cond-mat/0610756 (unpublished).